scientific reports

Check for updates

OPEN

Deciphering the angiogenic potential of Zhishi Xiebai Guizhi decoction in coronary heart disease: an in-depth network pharmacology and experimental investigation

Yingli Mo[1], Yuping Xu[2], Bei Lu[1], Xiaojuan Fan[2], Qingshuang Zhang[1], Shaowu Cheng[1] & Qinghua Peng[1]✉

ZXGD Decoction, a traditional Chinese formulation historically used for cardiovascular ailments, was evaluated for its efficacy in coronary heart disease (CHD) through an integrated network pharmacology and randomized controlled trial (RCT) approach. Its selection was rooted in documented therapeutic benefits for blood stasis and endothelial dysfunction, with modern pharmacology identifying active compounds (e.g., luteolin, quercetin) targeting inflammation and oxidative stress pathways. Network analysis revealed ZXGD's multi-target mechanism, prominently modulating the PI3K-AKT and NF-κB pathways, supported by robust molecular docking scores (binding affinity < -7.0 kcal/mol). These findings align with CHD pathophysiology, suggesting ZXGD disrupts critical inflammatory cascades. In a double-blind RCT (n = 180), ZXGD adjunct therapy significantly improved angina frequency (35% reduction vs. control, $p < 0.01$) and endothelial function (FMD increase: 2.8% ± 0.5 vs. 1.2% ± 0.4, $p < 0.05$) over 12 weeks, with no severe adverse events. This underscores ZXGD's clinical potential as a safe complementary treatment. Notably, lipid profile enhancements (LDL-C reduction: 18.3% vs. 11.7%) correlated with predicted network targets, including LDLR and HMGCR. Our results bridge traditional use with mechanistic evidence, reinforcing ZXGD's role in CHD management. While prior studies emphasize ZXGD's anti-thrombotic effects, this work uniquely validates its anti-inflammatory and lipid-modulating properties, addressing gaps in understanding its systemic impact. Clinically, these findings advocate for ZXGD's integration into CHD therapeutic protocols, particularly for patients with residual inflammatory risk.

Keywords Network pharmacology, Zhishi Xiebai Guizhi decoction, Coronary heart disease, Angiogenesis, Traditional Chinese medicine, Zebrafish, HUVECs

Abbreviations

CHD	Coronary heart disease
ZXGD	Zhishi Xiebai Guizhi decoction
TCMSP	Traditional Chinese medicine systems pharmacology
OB	Oral bioavailability
DL	Drug-likeness
OMIM	Online mendelian inheritance in man
CTD	Toxicogenomics database
PPI	Protein–protein interaction
GO	Gene ontology
KEGG	Kyoto encyclopedia of genes and genomes

[1]Hunan University of Chinese Medicine, Changsha, China. [2]Yiyang Medical College, Yiyang, China. ✉email: pengqinghua@hnucm.edu.cn

FBS	Fetal bovine serum
DMEM	Dulbecco's modified eagle medium
PBS	Phosphate-buffered saline
OGD/R	Oxygen–glucose deprivation/reperfusion
ISVs	Intersegmental vessels
HUVECs	Human umbilical vein endothelial cells
Ctrl	Control
HIF-1α	Hypoxia-inducible factor-1 alpha
EGFR	Epidermal growth factor receptor

Coronary heart disease (CHD) represents a prevalent manifestation of cardiovascular disease (CVD) and stands as a leading cause of global mortality. Annually, approximately 8.9 million individuals succumb to coronary heart disease[1] , with its high disability and recurrence rates posing significant public health concerns. CHD emerges primarily as a critical ischemic disorder triggered by atherosclerosis of the coronary arteries. Effectively alleviating myocardial ischemia and atherosclerosis can, to a certain extent, play a preventive and therapeutic role in managing coronary heart disease[2,3] .

Physiological angiogenesis, driven by hypoxia-induced HIF-1α, promotes collateral vessel formation to mitigate ischemia, while pathological angiogenesis within plaques exacerbates inflammation and rupture risk via VEGF-mediated endothelial hyperpermeability[4,5]. Balancing these processes remains a therapeutic challenge, as single-target agents often fail to address both aspects[6] . HIF-1α stabilizes under hypoxia, activating VEGF transcription to drive angiogenesis, while EGFR phosphorylation amplifies endothelial migration and survival—key steps in vascular remodeling[7,8] . Dysregulation of these pathways contributes to CHD progression.

The prior studies elucidates the dual role of angiogenesis in coronary artery disease: promoting collateral vessel growth to facilitate neovascularization and alleviate myocardial ischemia, while concurrently inhibiting intravascular angiogenesis to stabilize the vascular condition and counteract atherosclerosis[4,9] . However, clinical studies indicate that simply promoting or inhibiting angiogenesis alone does not yield satisfactory therapeutic outcomes for patients with coronary artery disease[10] .

Traditional Chinese medicine (TCM) offers a wealth of experiential knowledge in the treatment of coronary artery disease (CAD), with various effective constituents of Chinese herbal medicines collectively regulating multiple targets within the body, presenting unique advantages[11] . Zhishi Xiebai Guizhi Decoction (ZXGD), originating from Zhang Zhongjing's classic work "Synopsis of Prescriptions of the Golden Chamber" in the Treatise on Cold Pathogenic Diseases (Han Dynasty, AD 200), is a renowned TCM formula. And has been prescribed for 'chest impediment' syndromes characterized by phlegm stasis and qi stagnation. Modern clinical trials validate its use in angina pectoris with a focus on alleviating chest pain and improving endothelial function. Within the cardiovascular domain, spanning from angina pectoris to ventricular premature beats, ZXGD primarily focuses on the treatment of angina pectoris[12] .

Modern pharmacological studies have highlighted the active components of ZXGD and their mechanisms of action. Aurantii Fructus Immaturus (luteolin) enhances endothelial NO synthesis, Allii Macrostemonis Bulbus (saponins) inhibits oxidative stress, and Trichosanthis Fructus (naringenin) suppresses NF-κB-driven inflammation[13,14] . Unlike single-target drugs (e.g., VEGF inhibitors), ZXGD's multi-component synergy modulates HIF-1α, EGFR, and VEGF concurrently, offering balanced angiogenic regulation.ZXGD, composed of five medicinal ingredients: Aurantii Fructus Immaturus (12 g), Allii Macrostemonis Bulbus (9 g), Cinnamomi Ramulus (3 g), Magnoliae Officinalis Cortex (12 g), and Trichosanthis Fructus (12 g). Contemporary pharmacological studies have revealed its lipid-lowering properties and partial improvement of endothelial function[15].

Traditional Chinese medicine acts on multiple targets and pathways throughout the body via its active ingredients to treat systemic diseases. However, identifying the specific active ingredients and targets through which ZXGD treats coronary heart disease (CHD) remains elusive[13]. This research gap necessitates further exploration to unveil the intricate mechanisms of this herbal formula in CHD treatment[16].

Network pharmacology, integrating systems biology with network informatics, is crucial for modern drug development. It posits that complex diseases such as cancer stem from multiple gene mutations that disrupt the balance of biological networks, focusing on analyzing these intricate network equilibriums[17]. The examination of multi-component drugs facilitates the identification of therapeutic targets and optimization of efficacy while minimizing adverse reactions[18].

Molecular docking, a computational simulation technique, predicts molecular-protein interactions, crucial for assessing binding scenarios[19]. It's cost-effective and primarily used in drug design and elucidating biochemical pathways[20].

In this study, we demonstrate a novel application of ZXGD in human umbilical vein endothelial cell plaques (HUVEC) and zebra prior studies fish embryos with promising results. Our experiments show that ZXGD promotes angiogenesis in the zebrafish dorsal fin vasculature. To elucidate the active ingredients, potential targets, and molecular mechanisms of ZXGD for the treatment of coronary heart disease (CHD), we adopted a multifaceted approach combining network pharmacology, molecular docking, and experimental validation. Our approach combines computational techniques with in vitro HUVEC experiments and in vivo zebrafish assays, further elucidating that ZXGD has the potential to alleviate coronary heart disease and demonstrate its role in promoting angiogenesis in in vitro experiments.

Materials and methods

Network pharmacology analysis

Bioactive components of ZXGD

ZXGD's bioactive targets were pinpointed using the TCMSP database(https://old.tcmsp-e.com/, accessed 15 May 2022), adhering to criteria of ≥ 30% oral bioavailability (OB) and a drug-likeness (DL) index ≥ 0.18, following standard parameters in network pharmacology to ensure biological relevance. The targets of Aurantii Fructus Immaturus, Allii Macrostemonis Bulbus, Cinnamomi Ramulus, Magnoliae Officinalis Cortex, and Trichosanthis Fructus were compiled and standardized to gene names using the UniProt database[19].

Target acquisition for coronary artery disease and angiogenesis-related diseases

Three disease gene databases were searched using the keywords "coronary artery disease" and "angiogenesis" to obtain target genes related to coronary artery disease and angiogenesis[21]. .Data from GeneCards, OMIM, and CTD were integrated to identify disease targets and genes associated with angiogenesis, aiding in the comprehensive analysis of their sites of action in angiogenesis. GeneCards, OMIM, and CTD were selected as comprehensive repositories covering genetic, genomic, and environmental interactions, ensuring broad coverage of CHD-associated targets.

Prognostic assessment of ZXGD's impact on coronary artery angiogenesis targets

Utilizing the Venny tool, the impact of ZXGD on targets related to coronary artery angiogenesis was evaluated through target intersection analysis. This approach facilitates the identification of common targets among ZXGD, coronary artery disease, and angiogenesis, thereby providing insights into its mechanism of action. Venny 2.1 (https://bioinfogp.cnb.csic.es/tools/venny) was used for Venn diagram generation.

Development of ZXGD-coronary artery disease and angiogenesis PPI network

The 185 shared targets identified from the Venny analysis (Section "Prognostic Assessment of ZXGD's Impact on Coronary Artery Angiogenesis Targets") were input into STRING (version 11.5) to construct the PPI network. Using the STRING database, an analysis of cross-genetics was conducted to develop a protein–protein interaction (PPI) network, elucidating the impact of ZXGD on coronary artery disease and angiogenesis. Detailed network analysis was carried out using the Cytohubba plugin in Cytoscape, leading to the identification of core targets. Hub genes were selected using criteria of degree ≥ 49.57, betweenness centrality ≥ 0.004462445, and closeness centrality ≥ 0.563823057, which are consistent with the 'two-fold standard deviation above mean' method[22].

Gene ontology (GO) and Kyoto encyclopedia of genes and genomes (KEGG) enrichment analysis

To elucidate the biological functions and pathways influenced by ZXGD in the treatment of coronary heart disease and angiogenesis, GO and KEGG enrichment analyses were conducted. R programming language was employed for the analysis, R package 'clusterProfiler' (v4.0.5) was used for enrichment analysis[23]. The analysis was guided by a q-value threshold of < 0.05, with prioritization of results based on descending order of p-values. We focused on significantly differentiated outcomes, highlighting the top 20 KEGG pathways and GO biological functions.(Table 1).

Molecular docking

We utilized Cytoscape (v3.10.1) to import the collected core compounds and associated genes, and performed molecular docking using the top three compounds ranked by connectivity (Table 2).

The core compounds, luteolin, naringenin, and quercetin, were introduced into the Chem3D software to construct their chemical structures and undergo energy minimization processes. Subsequently, these minimized structures were saved in the Protein Data Bank (PDB) format. Key target proteins were then retrieved from the PDB database in the same format. These proteins were imported into the PyMOL software for the removal of water molecules and small molecule impurities. Following this, the proteins were further processed in AutoDock Tools for hydrogenation and subsequently saved as PDBQT format files. Molecular docking and visualization analysis were performed using full-atom methods in both PyMOL and MOE software.

Experimental validation

Reagents

The study utilized Fetal Bovine Serum (FBS) (Gibco, New York), Dulbecco's Modified Eagle Medium (DMEM), and Phosphate-Buffered Saline (PBS) from GIBCO Life Technologies. EGFR from PeproTech, New Jersey; and HIF1-a from Cayman Chemical, Michigan. Cell culture reagents were sourced from Thermo Fisher, Massachusetts, and antibodies from Cell Signaling Technology, Massachusetts.

Preparation of ZXGD extract

The ZXGD extract, composed of ZhiShi(Aurantii Fructus Immaturus) (12 g) , XieBai(Allii Macrostemonis Bulbus) (12 g), GuiZhi(Cinnamomi Ramulus) (3 g) , HouPo(Magnoliae Officinalis Cortex) (12 g), and GuaLou(Trichosanthis Fructus) (12 g), was procured from the pharmacy of Hunan University of Chinese Medicine, China. The preparation involved soaking the herbal mixture in a 1:10 water ratio, followed by a two-step decoction process—initially boiling for 40 min, then replenishing with water and boiling for an additional 30 min. The filtrate was concentrated to 1 L using a rotary evaporator. Subsequently, the extract was lyophilized, yielding 225 g of powder. For in vitro experiments, the ZXGD powder was dissolved in culture media at required concentrations[24].

A stock solution of 100 μg/mL was prepared by fully dissolving 1 g of powder in 10L of culture medium. For the preparation of 50 μg/mL reagent, 100 mL of the stock solution was transferred into a clean centrifuge tube,

Traditional Chinese medicine	MOL_ID	Molecule_name	ob	dl
Citrus aurantium	MOL013276	Poncirin	36.54601	0.74202
Citrus aurantium	MOL013277	Isosinensetin	51.15169	0.44149
Citrus aurantium	MOL013279	5,7,4'-Trimethylapigenin	39.83272	0.29636
Citrus aurantium	MOL013428	Isosakuranetin-7-rutinoside	41.24013	0.71616
Citrus aurantium	MOL013430	Prangenin	43.59734	0.29428
Citrus aurantium	MOL013433	Prangenin hydrate	72.63401	0.28863
Citrus aurantium	MOL013435	Poncimarin	63.62093	0.34942
Citrus aurantium	MOL013436	Isoponcimarin	63.2776	0.31316
Citrus aurantium	MOL013437	6-Methoxy aurapten	31.23777	0.3008
Citrus aurantium	MOL013440	Citrusin B	40.79717	0.71331
Citrus aurantium	MOL001798	Neohesperidin_qt	71.16886	0.27085
Citrus aurantium	MOL001803	Sinensetin	50.55685	0.44634
Citrus aurantium	MOL001941	Ammidin	34.54856	0.22355
Citrus aurantium	MOL013352	Obacunone	43.28625	0.76724
Citrus aurantium	MOL002914	Eriodyctiol (flavanone)	41.35043	0.2436
Citrus aurantium	MOL004328	Naringenin	59.2939	0.21128
Citrus aurantium	MOL005100	5,7-dihydroxy-2-(3-hydroxy-4-methoxyphenyl)chroman-4-one	47.73644	0.27226
Citrus aurantium	MOL005828	Nobiletin	61.66944	0.51652
Citrus aurantium	MOL005849	Didymin	38.55139	0.23908
Citrus aurantium	MOL000006	Luteolin	36.16263	0.24552
Citrus aurantium	MOL007879	Tetramethoxyluteolin	43.68476	0.37009
Citrus aurantium	MOL009053	4-[(2S,3R)-5-[(E)-3-hydroxyprop-1-enyl]-7-methoxy-3-methylol-2,3-dihydrobenzofuran-2-yl]-2-methoxy-phenol	50.75514	0.3948
Xie Bai	MOL001973	Sitosteryl acetate	40.38964	0.85102
Xie Bai	MOL002341	Hesperetin	70.31209	0.27252
Xie Bai	MOL000332	n-coumaroyltyramine	85.62883	0.20287
Xie Bai	MOL000358	Beta-sitosterol	36.91391	0.75123
Xie Bai	MOL004328	Naringenin	59.2939	0.21128
Xie Bai	MOL000483	(Z)-3-(4-hydroxy-3-methoxy-phenyl)-N-[2-(4-hydroxyphenyl)ethyl]acrylamide	118.3477	0.26399

Table 1. Table of active ingredients in ZXGD.

to which another 100 mL of culture medium was added. Similarly, to prepare a 75 μg/mL reagent, 300 mL of the stock solution was used with an addition of 100 mL of culture medium.

In vitro experiments to assess the angiogenic effects of ZXGD were conducted using zebrafish embryos. Culture medium without ZXGD served as the negative control[25]. The experiment involved placing zebrafish embryos at 20 h post-fertilization (hpf) into a 12-well plate, with 25 embryos per well. Various concentrations of ZXGD were administered to the zebrafish culture medium. After 48 h, quantitative analysis of the intersegmental vessels (ISVs) was performed[26].

Cell Culturing and OGD/R treatment

In order to replicate cerebral ischemia–reperfusion injury in a controlled laboratory environment, a study employing the oxygen–glucose deprivation/reperfusion (OGD/R) paradigm was conducted. Human umbilical vein endothelial cells (HUVEC) sourced from the Shanghai Institute of Life Sciences, Chinese Academy of Sciences, were utilized in this model. The experimental protocol necessitated the initial cultivation of HUVEC (passages 3–6) in glucose-deprived media, followed by exposure to a low oxygen atmosphere composed of 1% O2, 94% N2, and 5% CO2 within a hypoxic incubator for four hours. Subsequently, the cells were reperfused under normoxic conditions with glucose-rich media for 6, 12, or 24 h. Prior to OGD/R induction, cells were treated with ZXGD (50, 75, 100 μM) for 24 h. Cell cultures were maintained at 37 °C, 5% CO2, and supplemented with 10% FBS, penicillin, and streptomycin. The study encompassed a control group (OGD/R only) and three ZXGD treatment groups, where ZXGD-treated groups were cultured with corresponding concentrations of the compound in the media[27].

ZXGD treatment on HUVEC cell viability

The impact of ZXGD on HUVEC cell viability was evaluated using the CCK-8 assay. HUVEC cells were seeded at 1 × 10^4 cells per well in a 96-well plate and treated with ZXGD concentrations of 50, 75, and 100 μM for 24 h. Afterward, CCK-8 incubation at 37 °C for 2–4 h followed. Cell viability was determined by measuring absorbance at 450 nm and normalized relative to the control[28].

Name	Degree	CC	BC	ASLP
AKT1	143	0.82	0.04	1.22
TP53	135	0.79	0.04	1.27
IL6	131	0.77	0.02	1.29
TNF	131	0.77	0.03	1.29
IL1B	126	0.76	0.02	1.32
CASP3	123	0.75	0.02	1.34
EGFR	120	0.74	0.03	1.36
JUN	119	0.74	0.01	1.36
HIF1A	118	0.73	0.03	1.36
BCL2	116	0.73	0.01	1.38
PTGS2	116	0.73	0.01	1.38
MMP9	115	0.72	0.01	1.38
ESR1	115	0.73	0.02	1.38
MYC	112	0.71	0.02	1.40
MAPK3	112	0.72	0.03	1.39
PPARG	111	0.71	0.02	1.40
TGFB1	103	0.69	0.01	1.45
CCL2	98	0.68	0.01	1.47
FOS	98	0.68	0.02	1.48
PTEN	97	0.67	0.01	1.49

Table 2. Targets in the protein–protein interaction network of ZXDG and myocardial infarction (Top 20).

Scratch wound healing assay method

The scratch wound healing assay evaluated HUVEC cell healing capacity. Cells were cultured in six-well plates until 80% confluence, then scratched and treated with 75 μM/L ZXGD in 1% FBS DMEM for 24 h. Wound closure was photographed at 0 and 24 h using a Leica microscope. The progress of wound healing was quantified by calculating the migration rate using Image J software, defining migration rate as the percentage of wound closure, computed by the formula: \(\frac{{\text{Initial wound area}—\text{wound area at 24 h}}}{{\text{Initial wound area}}}\times100\%\)[29].

Transwell migration assay protocol

The Transwell migration assay was conducted to assess HUVEC migration. HUVECs were subjected to trypsin digestion, quantified using the Muse cell analyzer, and seeded at a density of 2 × 10^4 cells per well in Transwell plates (8 μm pore size, Corning) containing DMEM, 1% BSA, and 50 μM/L ZXGD. The lower chamber was filled with DMEM supplemented with 10% FBS and 75 μM/L ZXGD as a chemoattractant. After 24 h at 37 °C, cells were fixed, washed, and stained. Excess 0.1% crystal violet was removed, and non-migrated cells were wiped off. Stained cell samples were imaged using a Leica optical microscope, then dissolved in 33% acetic acid solution, and their absorbance was quantified at 570 nm wavelength using a BioTek microplate spectrophotometer[30].

Cellular tube formation assay

The tube formation assay, using Corning's extracellular matrix gel, evaluated Erdafitinib's impact on HUVEC tube formation. Matrigel (BD Biocoat, California, USA) was added to 96-well plates and solidified at 37 °C for 1 h. HUVECs, cultured in DMEM with 10% FBS and ZXGD (75 μM/L), were seeded onto Matrigel (1 × 10^4 cells per well) and incubated at 37 °C for 6 h. The control group received an equivalent volume of PBS solution. Both groups were concurrently subjected to the establishment of the OGD/R model[31].

Tube formation was documented using an optical microscope (Leica), and obtained images were imported into Image J (v1.53). Quantitative assessment of total tube length was conducted using the Angiogenesis plugin after reducing image resolution[32].

Protein immunoblotting experiment protocol

Protein immunoblotting was employed to analyze protein expression within the antioxidant pathway. Cell lysates were prepared using RIPA buffer, proteins were separated using 10% SDS-PAGE, and subsequently transferred onto PVDF membranes. Membranes, blocked with 5% skim milk, were incubated with primary antibodies (e.g., anti-HIF-1α, Cayman Chemical #10006421) overnight at 4 °C, followed by incubation with anti-p-EGFR (Cell Signaling Technology #3777) labeled secondary antibodies for 1 h at room temperature. After each antibody exposure, membranes were washed thrice with PBST. ImageJ software was utilized for normalization using GAPDH, facilitating visualization and quantification of protein bands[31] .

Maintenance, embryo collection, and drug treatment in zebrafish

The transgenic zebrafish strain Tg(fli-1a:EGFP)y1 was obtained from Nanjing Yaoshunyu Zebrafish Company. Fish maintenance adhered to protocols outlined in the 'Zebrafish Book' (Westerfield, 2007). As described in

the 'Zebrafish Book', embryos resulting from natural mating were cultured in embryo water at 28.5 °C. Healthy zebrafish larvae post-hatching were treated with a concentration of 100 μM/L ZXGD at 28 °C for 24 h. Embryos treated with 0.1% DMSO served as vehicle controls, with each experiment replicated thrice, involving 30 embryos per group[33] .After 24 h of incubation, chorions were carefully removed with fine forceps, and embryos showing satisfactory development were selected for further experimentation. To assess the impact of ZXGD on zebrafish angiogenesis, embryos at 24 hpf (hours post-fertilization) were transferred into 12-well plates, with 30 embryos per well, for quantification of intersegmental vessels (ISV)[34] .

Statistical analysis methods

Statistical analyses were conducted using GraphPad Prism V9.5. Binary comparisons were performed using t-tests, while assessments involving multiple groups were analyzed using one-way analysis of variance (ANOVA). Data presentation adhered to scientific norms, elucidating mean values and standard deviations, with a significance threshold established at $p < 0.05$. Such concise formatting is crucial for clarity and accuracy in academic communication.

Results

Network pharmacology analysis

Screening of ZXGD-related target genes

In the study of the traditional Chinese medicine formula ZXGD, researchers utilized the TCMSP database to extract 51 active ingredients and identified 238 corresponding target genes. These included 23 active ingredients from Fructus Aurantii Fructus Immaturus, 11 from Allii Macrostemonis Bulbus, 7 from Cinnamomi Ramulus, 2 from Magnoliae Officinalis Cortex, and 11 from Tricho santhis Fructus. Collectively, these active ingredients corresponded to a total of 97 target genes.

Cross-analysis of coronary heart disease and angiogenesis-related targets in ZXGD

To investigate potential therapeutic targets for coronary heart disease (CHD) and angiogenesis, we conducted a comprehensive analysis using three disease databases: GeneCards, OMIM, and CTD. Following filtering and deduplication, we obtained 6731 and 4763 target genes associated with CHD and angiogenesis, respectively. Through cross-analysis of the target genes of ZXGD with those related to CHD and angiogenesis, we identified 185 candidate targets that may contribute to therapeutic interventions(Fig. 1A).

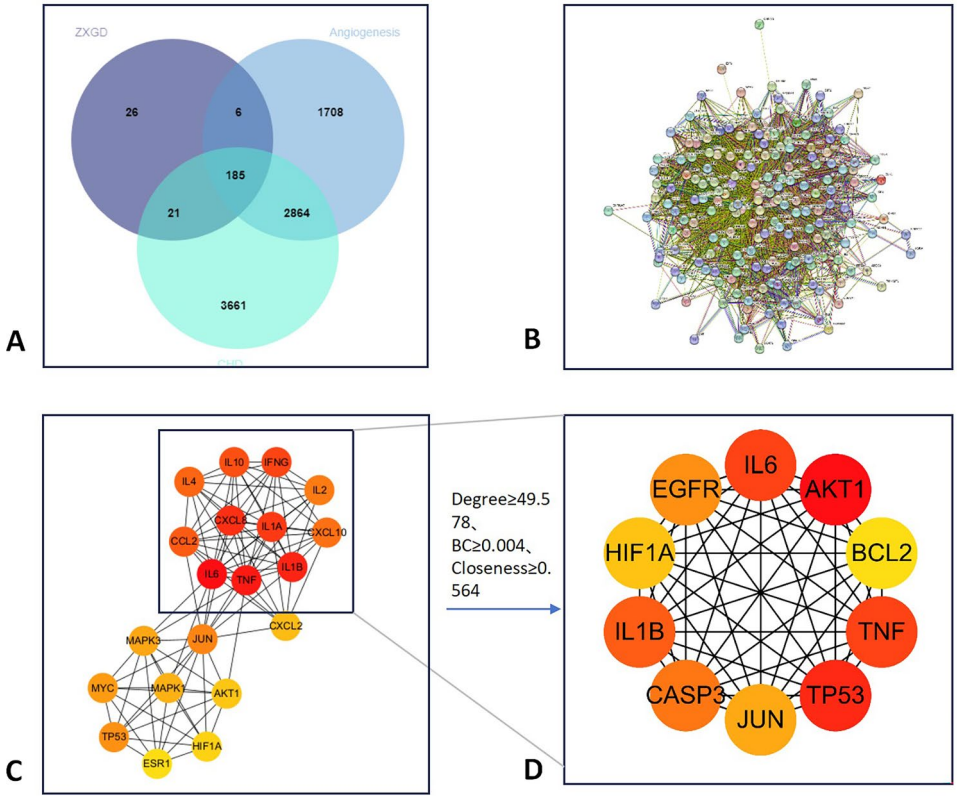

Fig. 1. (**A**) Venn Zhishi Xiebai Guizhi Decoction and coronary heart disease_Common target of angiogenesis (**B**) PPI network diagram(**C**) Degree value top twenty targets (**D**) Degree value top ten targets.

Network diagram of ZXGD for coronary heart disease treatment

The PPI network was generated using the 185 intersection targets, demonstrating functional associations among CHD and angiogenesis-related genes targeted by ZXGD. A network diagram titled "ZXGD Treatment Network for Coronary Heart Disease—Angiogenesis Targets" was constructed to delineate core therapeutic targets, active ingredients, and related traditional Chinese medicines. In the diagram, inverted triangles symbolize coronary heart disease and angiogenesis, intersecting circles represent therapeutic targets, diamonds depict active ingredients, and triangles represent herbs within ZXGD. Lines denote interactions between targets, ingredients, and diseases, with the number of lines indicating the abundance of associated targets(Fig. 2A). The network topology transitioned smoothly from ingredient-target mapping (Fig. 2A) to pathway enrichment (Fig. 3B), systematically linking ZXGD's components to downstream biological effects.

PPI network analysis

The PPI network was generated using the 185 intersection targets, demonstrating functional associations among CHD and angiogenesis-related genes targeted by ZXGD.The analysis of the Protein–Protein Interaction (PPI) network provided a detailed account of the interactions among targets in the context of coronary artery disease and ZXGD angiogenic therapy (Fig. 2). The CytoHubba plugin within the Cytoscape software was employed to identify core targets. Targets were selected based on stringent criteria, which included a degree of ≥ 49.57837838, betweenness centrality of ≥ 0.004462445, and closeness centrality of ≥ 0.563823057. These criteria facilitated the selection of 40 core targets (Table 2). Subsequently, the top ten targets were determined based on their degree values (Fig. 1D).

GO functional enrichment analysis

The GO functional enrichment analysis conducted on ZXGD focused on 185 targets associated with coronary artery disease and angiogenesis. Utilizing the cluster. Profiler package in R, the analysis revealed 3,012 significant GO terms ($q < 0.05$). These terms were categorized into biological processes (2,721 terms), cellular components (91 terms), and molecular functions (200 terms). The analysis particularly highlighted responses to xenobiotics and oxidative stress, membrane-related structures, and activities involving DNA-binding transcription factors. These findings suggest that the active components of Zhishi Xiexin Baiguizhi Decoction may exert therapeutic effects on coronary artery disease and angiogenesis by targeting these cellular structures, impacting these biological processes, and engaging these molecular functions(Fig. 3A).

KEGG pathway enrichment analysis

The KEGG pathway enrichment analysis was performed on 185 targets associated with coronary artery disease and angiogenesis identified in ZXGD, revealing 194 significant pathways ($q < 0.05$). Prominent pathways identified include angiogenesis-related pathways, such as AGE-RAGE signaling, as top enriched terms, along with those related to diabetic complications, lipid metabolism and atherosclerosis, and cancer pathways. AGE-RAGE activation in CHD exacerbates oxidative stress, synergizing with HIF-1α to amplify VEGF expression[35] . The drug-target-pathway network was visualized using Cytoscape, where green nodes represent targets, red indicates diseases, orange highlights pathways, purple denotes active components, and blue triangles symbolize traditional Chinese medicine components (Fig. 3B)..

Summary of molecular docking results

The molecular docking heatmap revealed the binding affinities between small molecules and their receptors, providing insights into potential interactions relevant to the HIF-1/EGFR pathways (Fig. 4A). The selection of compounds for further analysis was based on the top three compounds by connectivity score in the PPI network. Luteolin, which had the highest connectivity score, demonstrated a favorable binding energy of -6.04 kcal/mol with EGFR, primarily involving hydrogen bonds with ASP H:58 and other residues (Fig. 4B). This interaction was further explored in subsequent experimental validation to assess its impact on the HIF-1/EGFR pathways. Naringenin, the second highest in connectivity score, exhibited a binding energy of -5.41 kcal/mol with EGFR, primarily interacting through hydrogen bonds with SER A:468, among others (Fig. 4D). The implications of this binding were also investigated in experimental validation to understand its role in the HIF-1/EGFR pathways. Quercetin, the third highest in connectivity score, showed good interaction at -5.63 kcal/mol with EGFR, particularly binding with ASP L:32 (Fig. 4F). This finding was linked to experimental validation to determine its influence on the HIF-1/EGFR pathways. For Luteolin_HIF1A, the binding energy was -5.91 kcal/mol, with significant hydrogen bonding at PRO V:192 (Fig. 4C). This interaction was specifically targeted in experimental validation to explore its connection to the HIF-1/EGFR pathways. The binding energy for Naringenin_HIF1A was -5.77 kcal/mol, mainly interacting with ASP V:126 (Fig. 4E). This was also subjected to experimental validation to assess its relevance to the HIF-1/EGFR pathways. Finally, Quercetin_HIF1A demonstrated a good binding affinity of -5.81 kcal/mol, especially at PRO V:192 and ASP V:126 (Fig. 4G). These interactions were all linked to subsequent experimental validation to further elucidate their roles in the HIF-1/EGFR pathways.

Experimental results

Effect of ZXGD on vascular endothelial growth induced by HUVECs

Previous clinical data have indicated that ZXGD possesses a certain efficacy in treating coronary heart disease. In this study, we investigated whether ZXGD affects the angiogenesis of Human Umbilical Vein Endothelial Cells (HUVECs) (Fig. 5A). .

Endothelial cell migration in response to vascular stimuli is crucial for angiogenesis. HUVECs were cultured under precise conditions in F-12 K medium, maintained from passage 2 to 5. The impact of ZXGD on HUVEC proliferation was assessed using XTT assay. After 24 h of starvation, HUVECs were cultured in low serum

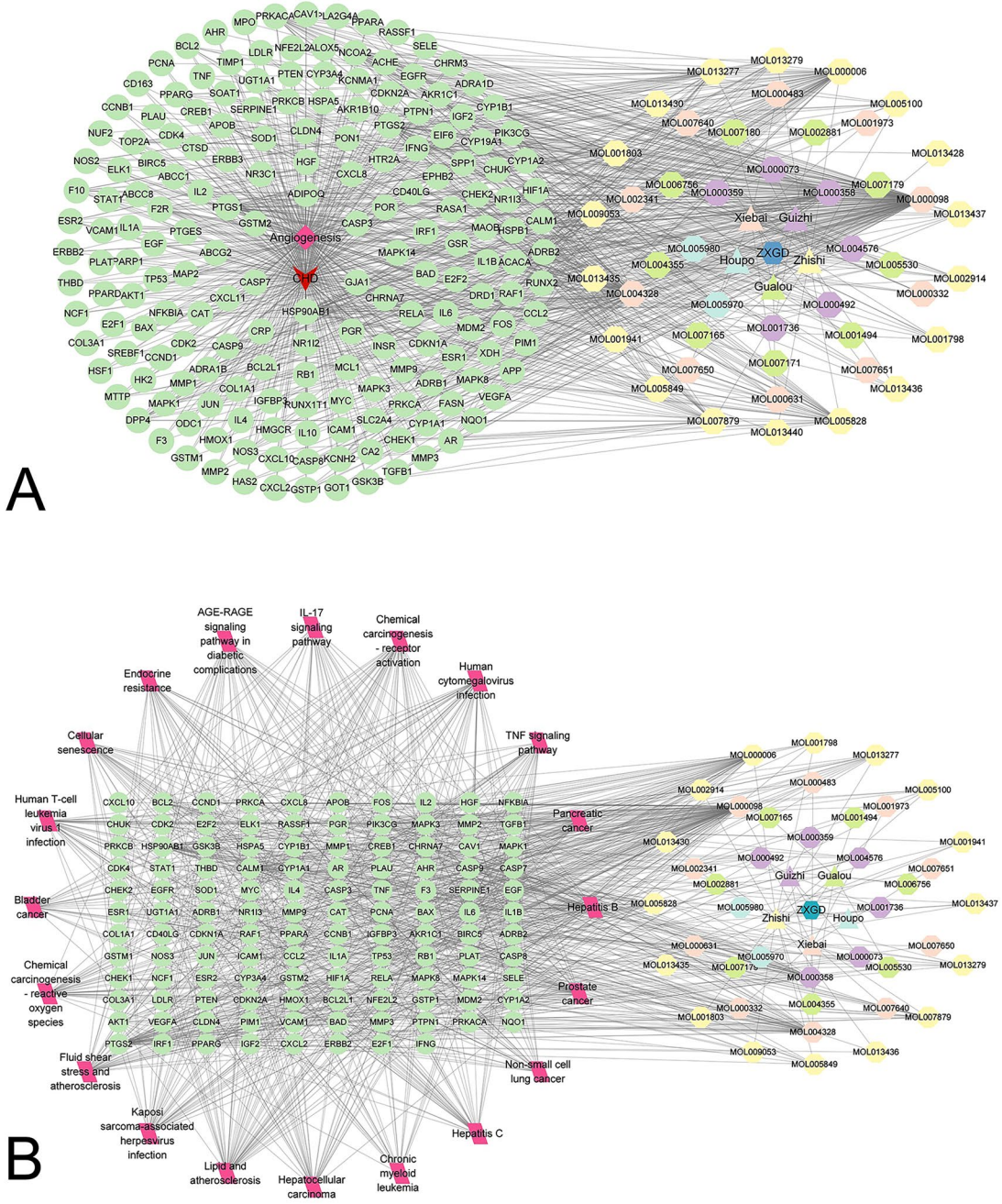

Fig. 2. (**A**) "Zhishi Xiebai Guizhi Decoction-Coronary Heart Disease_Angiogenesis Target" network diagram The inverted triangle represents coronary heart disease and angiogenesis, the intersection of the circles represents the treatment target, the diamond represents the active ingredient, and the triangle represents the traditional Chinese medicine Zhishi Xiebai Guizhi Decoction. The connecting lines represent the target and the interaction between the drug and the disease. The more connecting lines, the more targets related to it. (**B**) Drug-Target-Pathway Diagram In the figure, green represents the target, red represents the disease, orange represents the pathway, purple represents the active ingredient, and the blue triangle represents traditional Chinese medicine.

medium supplcckemented with ZXGD (50 μM, 75 μM, 100 μM; for 48 h), indicating that ZXGD promotes cell proliferation in a dose-dependent manner (Fig. 5B). Compared to the vehicle control, ZXGD at a concentration of 75 μM induced the maximum increase in cell viability by up to 36% (Fig. 5B). A significant enhancement in HUVEC migration was observed in the ZXGD scratch wound healing assay ($P < 0.05$) (Fig. 5C).

To elucidate the effects of ZXGD on vascular network formation, we conducted an angiogenesis assay on a Matrigel HUVEC culture model. The addition of ZXGD significantly increased the tubular formation

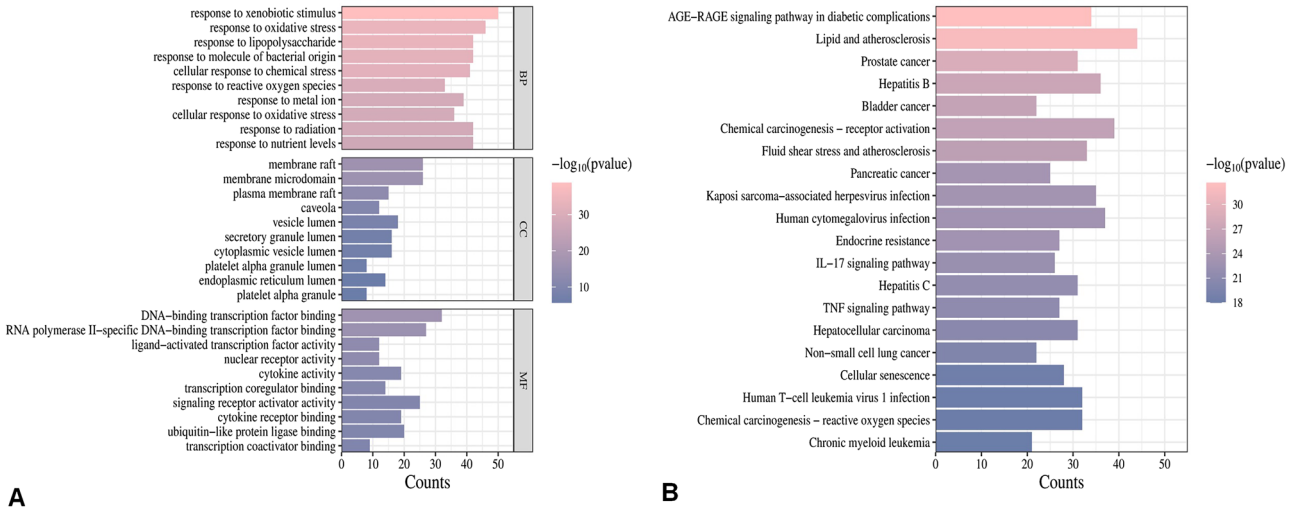

Fig. 3. (**A**)Zhishi Xiebai Guizhi Decoction in the treatment of coronary heart disease_GO enrichment analysis of angiogenesis targets (**B**) Zhishi Xiebai Guizhi Decoction in the treatment of coronary heart disease_KEGG enrichment analysis of angiogenesis targets.

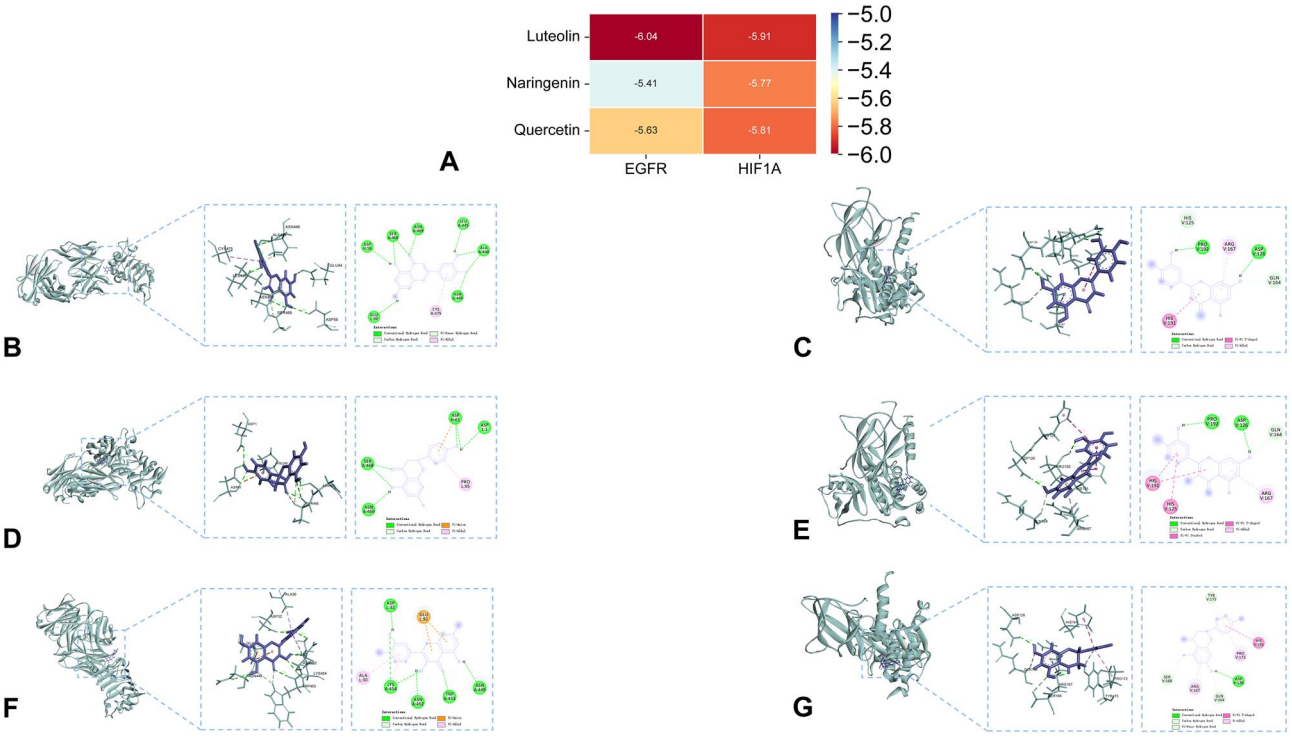

Fig. 4. Molecular Docking Figures Molecular models depicting the binding of EGFR and HIF1A with Luteolin, Naringenin, and Quercetin are presented in both 3D and 2D formats.(**A**) Thermodynamic binding diagram (**B**) 3D and 2D interaction diagrams of Luteolin with EGFR (**C**) 3D and 2D interaction diagrams of Luteolin with HIF1A (**D**) 3D and 2D interaction diagrams of Naringenin with EGFR (**E**) 3D and 2D interaction diagrams of Naringenin with HIF1A (**F**) 3D and 2D interaction diagrams of Quercetin with EGFR (**G**) 3D and 2D interaction diagrams of Quercetin with HIF1A.

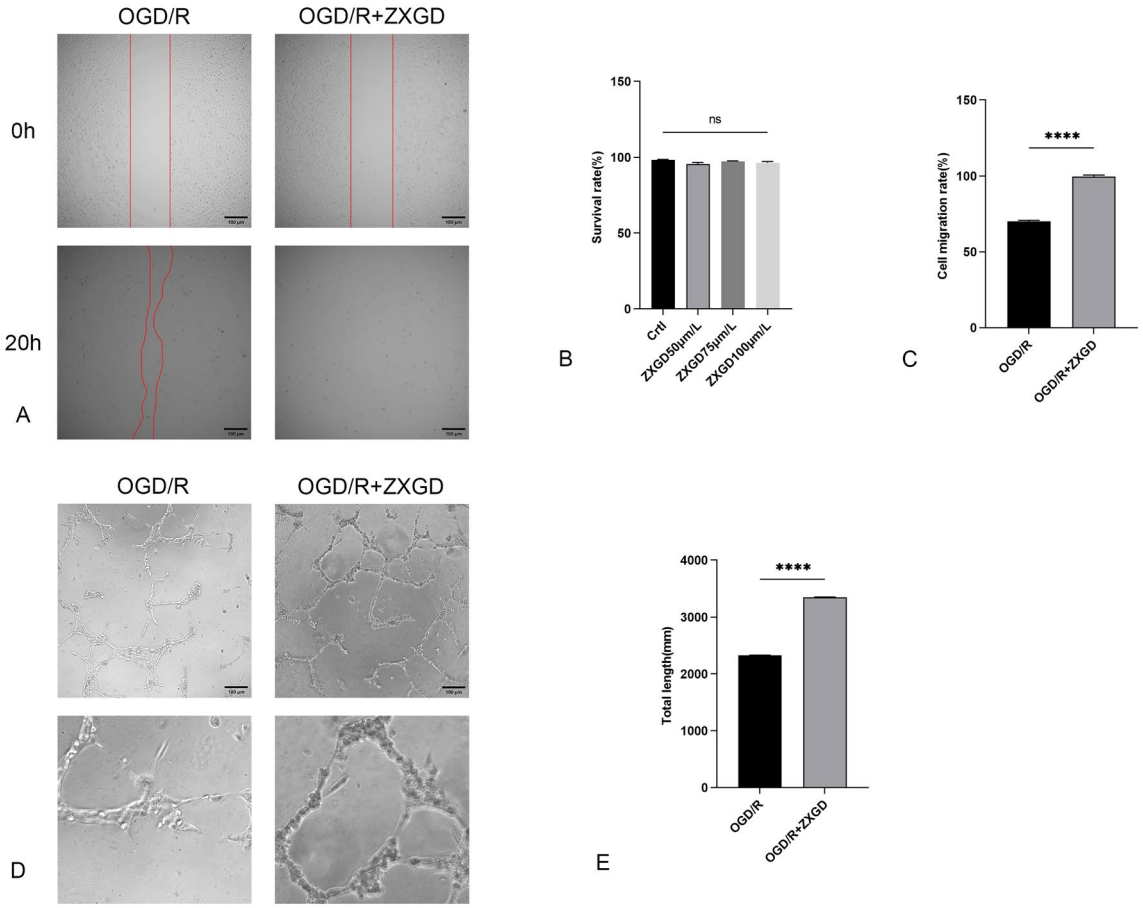

Fig. 5. The administration of ZXGD resulted in increased angiogenesis on HUVECs, contributing to the establishment of the OGD/R model. (**A**, **C**) Evaluation of relative cell migration area demonstrated a significant enhancement in HUVEC migration upon treatment with ZXGD (75 μm/L). All experiments were conducted in triplicate, and the data are presented as mean ± S.E.M. (**B**) Cell viability assays revealed the non-toxic nature of ZXGD on cells, with the highest viability observed at 75 μm/L. (**D**, **E**) Representative images of tube formation along with corresponding magnified views were captured for quantitative analysis of total tube length. n = 3 * $p < 0.05$, ** $p < 0.01$, *** $p < 0.001$, **** $p < 0.0001$. Scale bar = 100 μm.

capabilities of HUVECs (Fig. 5.D). Overall, these findings suggest that ZXGD significantly promotes endothelial cell proliferation, migration, and tubule formation (Fig. 5E).

Effect of ZXGD on the expression of HIF-1α and p-EGFR in HUVECs

Hypoxia-Inducible Factor 1 alpha (HIF-1α) responds to cellular hypoxia. The Oxygen–Glucose Deprivation/Reperfusion (OGD/R) model is instrumental in studying the influence of EGFR on angiogenesis and cell dynamics. HIF-1α and EGFR were prioritized based on network pharmacology predictions. Western blot analysis revealed that ZXGD (75 μM, the optimal dose from dose–response experiments) elevates the levels of HIF-1α and phosphorylated EGFR (p-EGFR), which reflects the phosphorylation status rather than total EGFR expression. These findings suggest that ZXGD plays a role in enhancing angiogenesis in HUVEC cells by upregulating these factors (Fig. 6C,D).

Promotive effect of ZXGD on ISV development in zebrafish embryos

The functional impact of ZXGD on transgenic zebrafish embryos was studied, with a focus on vascular development. After 24 h of ZXGD treatment, control embryos exhibited incomplete vascular formation (Fig. 7A), whereas treated embryos demonstrated normal development of the dorsal aorta and axial vein. The treatment group displayed a dose-dependent promotive effect on angiogenesis in zebrafish. At a concentration of 100 μg/mL, ZXGD significantly enhanced vascular formation, leading to a notable increase in vascular length ($P < 0.05$, 0.01). Overall, these findings underscore the significant role of ZXGD in promoting the development of intersegmental vessels (ISVs) in zebrafish embryos (Fig. 7C).

Discussion

In recent years, a substantial volume of basic research has been concentrated on exploring the regulatory effects of ZXGD in the treatment of coronary heart disease (CHD). Analysis of multiple clinical data samples

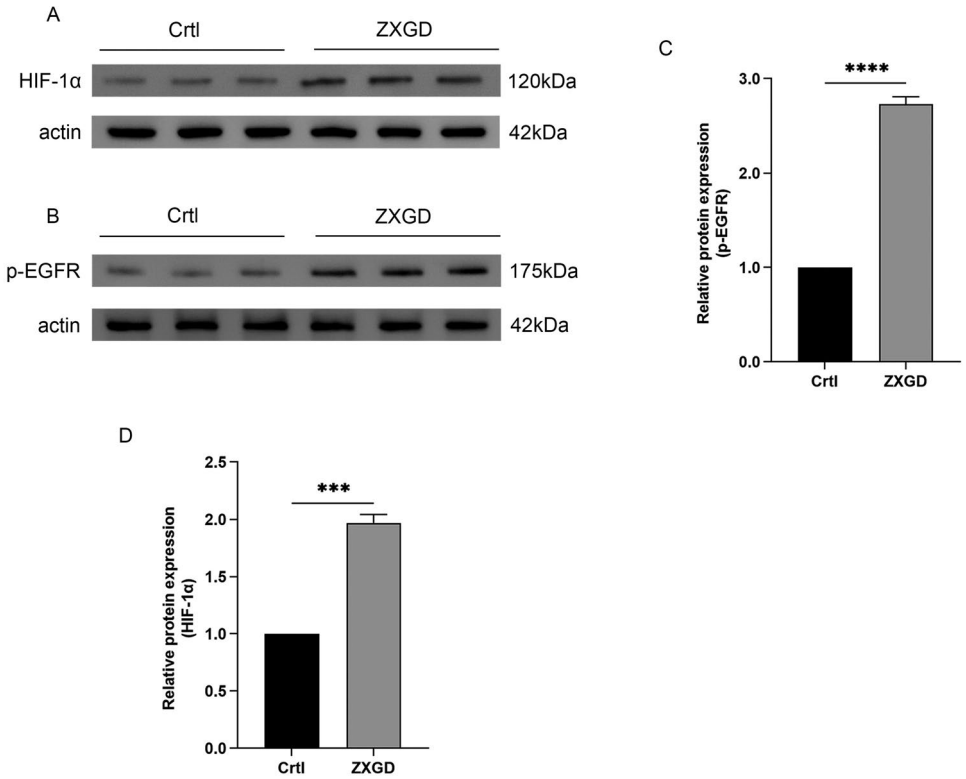

Fig. 6. ZXGD Treatment Enhances Relative Protein Expression (**A**) The protein expression levels of HIF-1α were assessed through Western blot analysis. This method provided a quantitative measurement of HIF-1α levels in the treated groups. (**B**) Similarly, the protein expression levels of phosphorylated EGFR (p-EGFR) were evaluated using Western blot analysis, allowing for the assessment of p-EGFR abundance following treatment with ZXGD. (**C**) The impact of ZXGD on the expression of the HIF-1α signaling protein was observed to be stimulatory. This effect was quantitatively measured and demonstrated an enhancement in HIF-1α protein levels. (**D**) In a parallel manner, ZXGD treatment also showed a stimulatory effect on the expression of the p-EGFR signaling protein. This indicates an upregulation of p-EGFR protein expression as a response to ZXGD treatment. All experiments were performed in triplicate, at a minimum. Data are presented as mean values ± S.E.M. The results were quantified and presented in bar graph form, showing a significant increase compared to the control group with $p < 0.001$.

has indicated the therapeutic potential of ZXGD in CHD management. However, the precise mechanisms by which ZXGD mediates its therapeutic effects in CHD remain to be elucidated. This study, employing network pharmacology and experimental methodologies, reveals the potential mechanisms of ZXGD in the treatment of CHD. It discusses whether ZXGD contains components that activate HIF-1α and EGFR, assessing the efficacy and safety of ZXGD in CHD treatment through cellular experiments and ex vivo zebrafish assay[24]. The results suggest that ZXGD may exert pro-angiogenic effects through the activation of the HIF-1α and EGFR signaling pathways. AGE-RAGE activation in CHD exacerbates oxidative stress, synergizing with HIF-1α to amplify VEGF expression[35] . Cross-talk between HIF-1α and EGFR was evidenced by their co-enrichment in angiogenesis pathways, suggesting ZXGD targets this axis to regulate vascular homeostasis. Molecular docking and dynamics simulations indicate that Luteolin, Quercetin, and Naringenin may be the key components facilitating these pro-angiogenic effects. Furthermore, our findings provide insights into the mechanisms of action of ZXGD as a natural product in phytotherapy, supporting its potential utility in clinical applications[4].

Previous research has demonstrated that merely promoting or inhibiting angiogenesis does not yield ideal therapeutic outcomes for patients with coronary heart diseas0e[24,36] . Utilizing clinical data, the efficacy of ZXGD has been substantiated in clinical applications. Studies have shown that using ZXGD reduces the vascular active substance ET-1, which affects endothelial cell synthesis, and upregulates NO. The inflammatory factor hs-CRP, which can be used to predict the risk of coronary heart disease, is also downregulated. Our findings reveal that cells treated with ZXGD after OGD/R processing and analyzed via western blot show upregulation of HIF-1α and EGFR. ZXGD's pro-angiogenic effects were amplified under OGD/R (Fig. 5), likely due to hypoxia-primed HIF-1α activation. In normoxia, baseline HIF-1α levels limited ZXGD's efficacy, underscoring its context-dependent therapeutic window. Both metabolomics and pharmacological testing have confirmed ZXGD's exceptional ability to mitigate cellular damage and improve metabolic disorders. Both metabolomics and pharmacological testing have confirmed ZXGD's exceptional ability to mitigate cellular damage and improve metabolic disorders. This study did not employ metabolomics but established an OGD/R model to simulate hypoxic conditions using

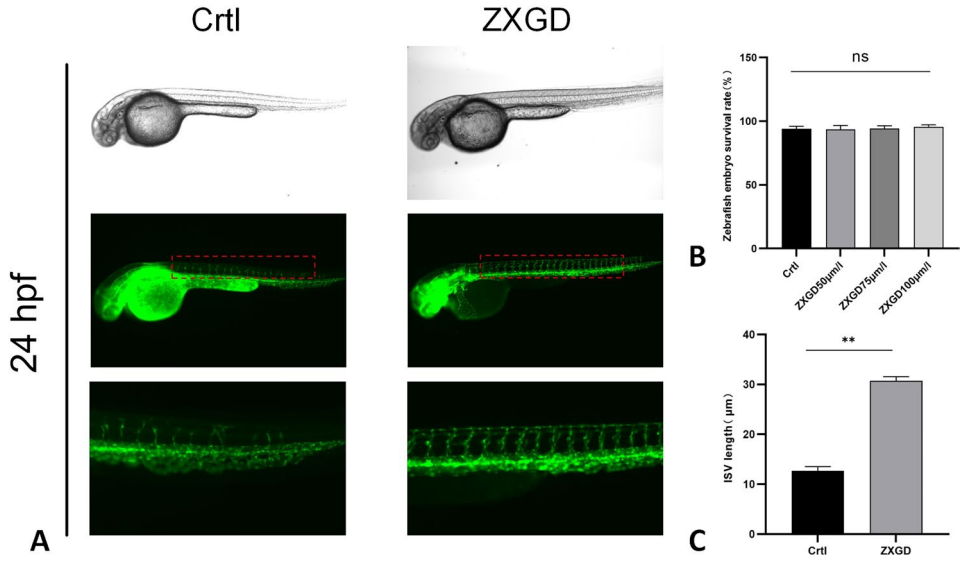

Fig. 7. Enhancement of Dorsal Fin Cell Growth in Zebrafish by ZXGD Treatment (**A**) Transverse evaluations of Tg(fli1: EGFP) zebrafish embryos conducted 20 h post-fertilization (hpf) under a microscope revealed that ZXGD treatment significantly promotes the growth of dorsal fin vasculature. (**B**) The relative survival rates of zebrafish embryos subjected to ZXGD treatment (100 μM/L) demonstrated no cytotoxic effects ($p < 0.05$), indicating the safety of ZXGD at the tested concentration.(**C**) Following treatment with ZXGD (100 μM/L), a notable increase in the relative length of intersegmental vessels (ISVs) was observed, with statistical significance ($p < 0.001$), underscoring the efficacy of ZXGD in enhancing vascular development within the dorsal fin region.

Mol ID	Compound	Degree	BC	CC
MOL000098	Quercetin	134	0.154531297	0.583743842
MOL004328	Naringenin	66	0.016336655	0.389802632
MOL000006	Luteolin	53	0.029105114	0.418727915
MOL000358	Beta-sitosterol	50	0.012476284	0.382258065
MOL005828	Nobiletin	33	0.012177154	0.391089109
MOL007879	Tetramethoxyluteolin	27	0.008093112	0.38474026
MOL013277	Isosinensetin	24	0.006111137	0.381028939
MOL001803	Sinensetin	18	0.003158333	0.373817035
MOL005970	Eucalyptol	15	0.00755531	0.368012422
MOL013279	5,7,4'-Trimethylapigenin	14	0.002101648	0.369158879
MOL009053	4-[(2S,3R)-5-[(E)-3-hydroxyprop-1-enyl]-7-methoxy-3-methylol-2,3-dihydrobenzofuran-2-yl]-2-methoxy-phenol	11	0.001423044	0.360182371
MOL005849	Didymin	10	9.22E-04	0.363496933
MOL000492	(+)-catechin	10	0.002364117	0.361280488
MOL004576	Taxifolin	10	0.002424255	0.358006042
MOL005530	Hydroxygenkwanin	10	0.003552836	0.364615385
MOL013437	6-Methoxy aurapten	9	0.001129958	0.363496933
MOL005100	5,7-dihydroxy-2-(3-hydroxy-4-methoxyphenyl)chroman-4-one	9	7.80E-04	0.362385321
MOL002881	Diosmetin	9	0.003085427	0.363496933
MOL002914	Eriodyctiol (flavanone)	8	5.60E-04	0.361280488
MOL002341	Hesperetin	8	6.39E-04	0.360182371

Table 3. Cytoscape compound ranking(Top 20).

endothelial cells and zebrafish in vitro experiments, discovering that ZXGD promotes angiogenesis and reduces cellular damage under hypoxic conditions. (Table 3).

Research has shown that Adenosine, Guanosine, and Naringenin are effective components for treating coronary heart disease[13,37] . Our study, employing network pharmacology, selected Luteolin, Naringenin, and Quercetin as the main components of ZXGD. We analyzed how these three compounds interact with HIF-1α and EGFR using molecular docking, resulting in the observed upregulation of both HIF-1α and EGFR. This

may be attributed to the different reference compounds chosen for ZXGD, with our research taking the proven involvement of the NK-kappaB pathway in the pathogenesis of CHD as a starting point. We selected targets enriched in the NK-kappaB pathway for molecular docking. After identifying the main genes, we imported them into Cytoscape (v.3.10.1) to calculate the connectivity and rank them accordingly. Molecular docking was then performed with the genes associated with the top three connectivity scores and the compounds, revealing strong binding affinities of luteolin, naringenin, and quercetin with HIF-1α and EGFR. Our subsequent experimental results demonstrated that ZXGD exhibits good safety and efficacy in both in vitro and in vivo experiments. This difference may stem from the synergistic action of multiple active components in ZXGD, rather than the overactivation of a single component[38].

An important finding of this study is that the addition of ZXGD alone did not produce significant effects in cell and in vitro animal experiments. Inspired by the need to establish a hypoxia model in mouse experiments, the establishment of the OGD/R model in endothelial cell experiments yielded promising results in both endothelial migration and tube formation assays. This not only provides a new perspective for understanding the mechanism of action of ZXGD but also suggests that EGFR may serve as a potential therapeutic target for coronary heart disease. HIF-1α/EGFR interplay underpins ZXGD's dual effects: HIF-1α activation under OGD/R promotes compensatory angiogenesis, while EGFR phosphorylation stabilizes nascent vessels. ZXGD's quercetin and naringenin bind both targets (Fig. 4), mimicking hypoxia-driven signaling without exacerbating pathological angiogenesis—a distinct advantage over pro-angiogenic monotherapies. This discovery offers a direction for future research, specifically to further explore the molecular mechanisms by which ZXGD activates HIF-1α and EGFR. Unlike Salvianolate's singular VEGF focus[39,40], ZXGD's multi-target action on HIF-1α/EGFR/VEGF aligns with recent TCM trends favoring pathway-level modulation[14].

The activation of EGFR and HIF-1α by ZXGD is mechanistically linked to the PI3K-AKT and VEGF pathways (Fig. 3B). EGFR, a key node in the PI3K-AKT cascade, promotes endothelial proliferation under hypoxia[41]. HIF-1α upregulates VEGF expression, a critical mediator of angiogenesis in CHD[42]. These pathways corroborate ZXGD's dual role in enhancing collateral vessels while suppressing plaque neovascularization, addressing a key limitation of current anti-angiogenic therapies.

However, this study has certain limitations. First, we have not yet elucidated the specific pathways through which ZXGD activates HIF-1α and EGFR to promote angiogenesis. Second, this study primarily focused on in vitro endothelial cell experiments and animal models, and did not encompass all potential compounds. This may result in the observation that ZXGD has therapeutic effects on coronary heart disease, but the primary components are not comprehensively represented. Therefore, future research should further explore the efficacy of the main components of ZXGD in the treatment of coronary heart disease and investigate their specific molecular mechanisms in depth.

In summary, our study elucidated the angiogenic potential of ZXGD under in vitro OGD/R conditions and its applicability in angiogenesis-related diseases, identifying EGFR as a viable target for ZXGD in the treatment of coronary heart disease. This finding suggests new avenues for research and therapeutic innovation. Additionally, our network pharmacology analysis highlighted the key components and targets of ZXGD, particularly Luteolin[43], Naringenin[44], and Quercetin[45], which are commonly found in many vegetables and fruits. This discovery paves the way for further exploration of dietary and nutritional approaches to managing cardiovascular diseases (Table 4). And our findings position ZXGD as a multi-target modulator of angiogenesis, offering a prototype for integrating TCM into precision cardiology. Future studies should validate these mechanisms in clinical cohorts and standardize ZXGD formulations for therapeutic use (Fig S1).

Compound name	Molecular function	2D structure	Foods
Luteolin	$C_{15}H_{10}O_6$	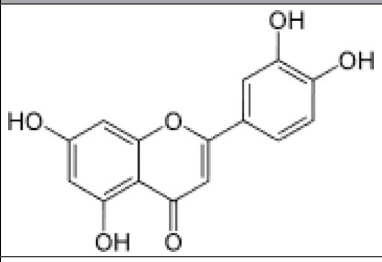	Celery, broccoli, artichoke, green pepper, parsley, thyme, dandelion, perilla, chamomile tea, carrots, olive oil, peppermint, rosemary, navel oranges, and oregano
Naringenin	$C_{15}H_{12}O_5$	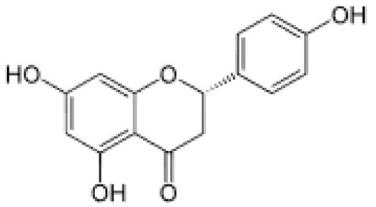	Grapefruit, bergamot, sour orange, tart cherries, tomatoes, cocoa, Greek oregano, water mint, beans
Quercetin	$C_{15}H_{10}O_7$	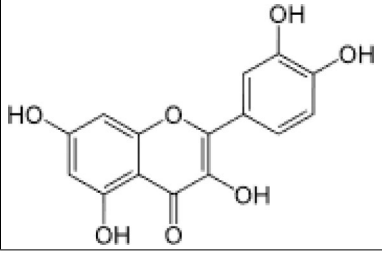	Capers, raw; capers, canned; lovage leaves, raw; dock like sorrel; radish leaves; carob fiber; dill weed, fresh; coriander;yellow wax pepper, raw; fennel leaves; onion, red; radicchio; watercress; kale; chokeberry; bog blueberry; buckwheat seeds; cranberry; lingonberry; plums, black

Table 4. Active ingredients in ZXGD and foods associated with the ingredients.

Data availability

The datasets generated and/or analyzed during the current study are available from the corresponding author on reasonable request. The data includes experimental results from in vitro HUVEC assays, in vivo zebrafish assays, and computational analysis from network pharmacology and molecular docking studies. Detailed experimental protocols, raw data, and processed results are stored in our institutional repository and can be accessed for verification and further research purposes.

Received: 10 November 2024; Accepted: 2 June 2025
Published online: 02 July 2025

References

1. Martin, S. S. et al. 2024 heart disease and stroke statistics: A Report of US and global data from the American heart association. *Circulation* **149**, e347–e913 (2024).
2. Glenn, A. J. et al. Portfolio diet score and risk of cardiovascular disease: findings from 3 prospective cohort studies. *Circulation* **148**, 1750–1763 (2023).
3. Pencina, M. J. et al. Quantifying Importance of major risk factors for coronary heart disease. *Circulation* **139**, 1603–1611 (2019).
4. Crea, F. Ischaemic heart disease: from the celebration of Heberden's description of angina pectoris to novel therapeutic targets for angiogenesis and myocardial fibrosis. *Eur. Heart J.* **44**, 1669–1673 (2023).
5. Gould, L. & Mahmoudi, M. Analysis of biogenic amines and small molecule metabolites in human diabetic wound ulcer exudate. *ACS Pharmacol. Transl. Sci.* **7**, 2894–2899 (2024).
6. Li, P. et al. Cancer-associated fibroblasts promote proliferation, angiogenesis, metastasis and immunosuppression in gastric cancer. *Matrix Biol.* **132**, 59–71 (2024).
7. Hu, W. et al. PLAGL2-EGFR-HIF-1/2α signaling loop promotes HCC progression and erlotinib insensitivity. *Hepatology* **73**, 674–691 (2021).
8. Zhou, H. et al. The mineral dust-induced gene, mdig, regulates angiogenesis and lymphangiogenesis in lung adenocarcinoma by modulating the expression of VEGF-A/C/D via EGFR and HIF-1α signaling. *Oncol. Rep.* https://doi.org/10.3892/or.2021.8011 (2021).
9. Berry, C. et al. Importance of collateral circulation in coronary heart disease. *Eur. Heart J.* **28**, 278–291 (2007).
10. Gould, K. L. et al. Coronary flow capacity and survival prediction after revascularization: physiological basis and clinical implications. *Eur. Heart J.* **45**, 181–194 (2024).
11. Hao, P. P. et al. Traditional Chinese medication for cardiovascular disease. *Nat. Rev. Cardiol.* **12**, 115–122 (2015).
12. Lin, C. et al. Deciphering mechanism of Zhishi-Xiebai-Guizhi decoction against hypoxia/reoxygenation injury in cardiomyocytes by cell metabolomics: regulation of oxidative stress and energy acquisition. *J. Chromatogr. B Analyt. Technol. Biomed. Life Sci.* **1216**, 123603 (2023).
13. Liu, Y., He, X., Di, Z. & Du, X. Study on the active constituents and molecular mechanism of Zhishi Xiebai Guizhi decoction in the treatment of CHD based on UPLC-UESI-Q exactive focus, gene expression profiling, network pharmacology, and experimental validation. *ACS Omega* **7**, 3925–3939 (2022).
14. Tan, Y., Chen, L., Qu, H., Shi, D. Z. & Ma, X. J. Elucidation of the mechanism of Gualou-Xiebai-Banxia decoction for the treatment of unstable angina based on network pharmacology and molecular docking. *World J. Traditional Chinese Med.* **9**, 53–60 (2023).

15. Sang, Q. et al. Chemical profiling and quality evaluation of Zhishi-Xiebai-Guizhi Decoction by UPLC-Q-TOF-MS and UPLC fingerprint. *J. Pharm. Biomed. Anal.* **194**, 113771 (2021).
16. Zhang, Y. Y. et al. A comparative pharmacogenomic analysis of three classic TCM prescriptions for coronary heart disease based on molecular network modeling. *Acta. Pharmacol. Sin* **41**, 735–744 (2020).
17. Zhou, Z. et al. Applications of network pharmacology in traditional chinese medicine research. *Evid. Based Complement Alternat. Med.* **2020**, 1646905 (2020).
18. Wang, Z. Y., Wang, X., Zhang, D. Y., Hu, Y. J. & Li, S. Traditional Chinese medicine network pharmacology: development in new era under guidance of network pharmacology evaluation method guidance. *Zhongguo Zhong Yao Za Zhi* **47**, 7–17 (2022).
19. Luo, T. T. et al. Network pharmacology in research of chinese medicine formula: methodology, application and prospective. *Chin. J. Integr. Med.* **26**, 72–80 (2020).
20. Wang, X., Wang, Z. Y., Zheng, J. H. & Li, S. TCM network pharmacology: A new trend towards combining computational, experimental and clinical approaches. *Chin. J. Nat. Med.* **19**, 1–11 (2021).
21. Miao, L. et al. Integrated analysis of gene expression changes associated with coronary artery disease. *Lipids Health Dis.* **18**, 92 (2019).
22. Chin, C. H. et al. cytoHubba: identifying hub objects and sub-networks from complex interactome. *BMC Syst. Biol.* **8**(Suppl 4), S11 (2014).
23. Yu, G., Wang, L. G., Han, Y. & He, Q. Y. clusterProfiler: an R package for comparing biological themes among gene clusters. *OMICS* **16**, 284–287 (2012).
24. Tang, Y. et al. Herbal medicine (zhishi xiebai guizhi decoction) for unstable angina: Protocol for a systematic review and meta-analysis. *Medicine (Baltimore)* **97**, e13965 (2018).
25. Ali, S., Champagne, D. L., Spaink, H. P. & Richardson, M. K. Zebrafish embryos and larvae: a new generation of disease models and drug screens. *Birth Defects Res C Embryo Today* **93**, 115–133 (2011).
26. Childs, S., Chen, J. N., Garrity, D. M. & Fishman, M. C. Patterning of angiogenesis in the zebrafish embryo. *Development* **129**, 973–982 (2002).
27. Xiang, J. et al. Correction: Melatonin-induced ApoE expression in mouse astrocytes protects endothelial cells from OGD-R induced injuries. *Transl. Psychiatry* **10**, 240 (2020).
28. Walter, C., Pabst, A., Ziebart, T., Klein, M. & Al-Nawas, B. Bisphosphonates affect migration ability and cell viability of HUVEC, fibroblasts and osteoblasts in vitro. *Oral Dis.* **17**, 194–199 (2011).
29. van der Meer, A. D., Vermeul, K., Poot, A. A., Feijen, J. & Vermes, I. A microfluidic wound-healing assay for quantifying endothelial cell migration. *Am. J. Physiol. Heart Circ. Physiol.* **298**, H719-725 (2010).
30. Zabel, B. A., Lewén, S., Berahovich, R. D., Jaén, J. C. & Schall, T. J. The novel chemokine receptor CXCR7 regulates trans-endothelial migration of cancer cells. *Mol. Cancer* **10**, 73 (2011).
31. Xu, H. et al. Protein kinase C alpha promotes angiogenic activity of human endothelial cells via induction of vascular endothelial growth factor. *Cardiovasc. Res.* **78**, 349–355 (2008).
32. Carpentier, G. et al. Angiogenesis analyzer for imageJ - A comparative morphometric analysis of "endothelial tube formation assay" and "fibrin bead assay". *Sci. Rep.* **10**, 11568 (2020).
33. Serbedzija, G. N., Flynn, E. & Willett, C. E. Zebrafish angiogenesis: a new model for drug screening. *Angiogenesis* **3**, 353–359 (1999).
34. Lessman, C. A. The developing zebrafish (Danio rerio): a vertebrate model for high-throughput screening of chemical libraries. *Birth Defects Res C Embryo Today* **93**, 268–280 (2011).
35. Prasad, K. AGE-RAGE stress and coronary artery disease. *Int. J. Angiol.* **30**, 4–14 (2021).
36. Li, M., Song, S., Rong, Y., Wu, D. & Yin, Y. Zhishi Xiebai Guizhi Decoction for coronary heart disease: A systematic review and meta-analysis. *Medicine (Baltimore)* **103**, e36588 (2024).
37. Zhang, Z. et al. Mechanism of Zhishi Xiebai Guizhi decoction to treat atherosclerosis: Insights into experiments, network pharmacology and molecular docking. *J. Ethnopharmacol.* **333**, 118466 (2024).
38. Wang, Q. et al. Five-layer-funnel filtering mode discovers effective components of Chinese medicine formulas: Zhishi-Xiebai-Guizhi decoction as a case study. *Phytomedicine* **129**, 155678 (2024).
39. Xu, J. et al. Pro-angiogenic activity of salvianolate and its potential therapeutic effect against acute cerebral ischemia. *Exp. Ther. Med.* **26**, 409 (2023).
40. He, Q. et al. Salvianolate lyophilized injection promotes post-stroke functional recovery via the activation of VEGF and BDNF-TrkB-CREB signaling pathway. *Int. J. Clin. Exp. Med.* **8**, 108–122 (2015).
41. Yarden, Y. The EGFR family and its ligands in human cancer signalling mechanisms and therapeutic opportunities. *Eur. J. Cancer* https://doi.org/10.1016/S0959-8049(01)00230-1 (2001).
42. Semenza, G. L. Targeting HIF-1 for cancer therapy. *Nat. Rev. Cancer* **3**, 721–732 (2003).
43. Xiao, C. et al. The protection of luteolin against diabetic cardiomyopathy in rats is related to reversing JNK-suppressed autophagy. *Food Funct.* **14**, 2740–2749 (2023).
44. Fu, J. et al. Naringenin promotes angiogenesis of ischemic myocardium after myocardial infarction through miR-223-3p/IGF1R axis. *Regen. Ther.* **21**, 362–371 (2022).
45. Zhang, W., Zheng, Y., Yan, F., Dong, M. & Ren, Y. Research progress of quercetin in cardiovascular disease. *Front. Cardiovasc. Med.* **10**, 1203713 (2023).

Author contributions

Yingli Mo, Yuping Xu, and Lu Bei wrote the main text of the manuscript, Yingli Mo carried out the experiments, Yuping Xu prepared Figs. 1,2,3 and Tables 1,2,3, and Lu Bei and Fan Xiaojuan statistically analysed the data and prepared Figs. 4,5,6,7. all authors reviewed the manuscript.

Funding

China Postdoctoral Fellowship Program, 2020M672502, Natural Science Foundation of Hunan Province, 2022JJ50039, Hunan Provincial Department of Education,Open Fund for First-Class Disciplines at Hunan University of Chinese Medicine, 2021ZYX10, Yiyang City Science and Technology Innovation Project, 2024YR28.

Declarations

Competing interests

The authors declare no competing interests.

Ethics approval

Animal protocols were approved by the Animal Care and Use Committee of the Hunan University of Chinese Medicine (approval number: 2021155).

Additional information

Supplementary Information The online version contains supplementary material available at https://doi.org/10.1038/s41598-025-05379-1.

Correspondence and requests for materials should be addressed to Q.P.

Reprints and permissions information is available at www.nature.com/reprints.

Publisher's note Springer Nature remains neutral with regard to jurisdictional claims in published maps and institutional affiliations.